Desalination and Water Treatment
www.deswater.com

doi: 10.1080/19443994.2013.822633

52 (2014) 6453–6463
October

Taylor & Francis
Taylor & Francis Group

Ferric hydroxide: preparation, characterisation and fluoride removal studies from water

M.G. Sujana*, S. Anand

Environment and Sustainability Department, CSIR-Institute of Minerals and Materials Technology, Bhubaneswar, India
Tel. +91 0674 2379417; Fax: +91 0674 2581160; email: mgsujana@gmail.com

Received 6 August 2012; Accepted 17 June 2013

ABSTRACT

The objective of this study is to investigate the fluoride removal efficiency of pure ferric hydroxide from aqueous solutions. The sample was synthesised through wet chemical route at optimised experimental conditions and was characterised by chemical, morphological and textural properties using transmission electron microscope, thermo gravimetry, X-ray diffraction, Brunauet–Emmett–Teller surface area and Fourier transform infrared spectroscopy techniques. Studied operational variables for batch adsorption were pH, contact time, initial F^- concentration, solution temperature and presence of foreign ions (chloride, sulphate, phosphate, arsenate, nitrate and carbonate in the concentration range of 0–25 mg/L). The kinetic data revealed that the adsorption of fluoride onto ferric hydroxide is a complex process involving surface adsorption along with ion exchange and interparticle diffusion as the rate-determining step. The equilibrium data fitted to both Langmuir and Freundlich isotherm models. The post-surface characterisation studies of fluoride adsorbed ferric hydroxide showed significant changes, and suggest the formation of new complexes on adsorbent surface. The regeneration (75–80%) and fluoride-contaminated groundwater treatment studies at natural pH are discussed in detail.

Keywords: Adsorption; Fluoride; Groundwater; Ferric hydroxide; Mechanism

---

1. Introduction

Fluoride exists in many forms, and the harmful nature of the fluoride is contingent upon the type of fluoride it is. Depending on its concentration, the fluoride in drinking water is known for both beneficial and detrimental effects on health, particularly to infants and young children. The toxicity of fluoride on human health is well documented [1]. According to the WHO guidelines and recommendations, in the areas with a warm climate, the optimal fluoride concentration in drinking water should remain below 1 mg/L, while in cooler climates it could go up to 1.2 mg/L. The differentiation derives from the fact that people perspire more in hot weather and consequently drink more water [2]. The Indian Standards for drinking water recommended maximum permissible limit of 1 mg/L and the maximum tolerance limit as 1.5 mg/L for potable water [3].

The conventional approaches for fluoride removal include chemical precipitation, ion exchange, adsorption, electro-dialysis, Donnan dialysis and reverse osmosis [4–7]. Among all these methods, adsorption technique is economically favourable and technically

---

*Corresponding author.

feasible to remove fluoride from aqueous solutions as the requirement of operative controls are minimal [8]. Activated alumina is one of the most widely used adsorbents for fluoride removal in the drinking water treatment due to its high affinity as aluminium ion can form inner-sphere complexation [9]. However, high activation cost and low adsorption capacity for fluoride by activated alumina inhibits its application. In this regard, lot of research work is going on to find out alternate, cost-effective and environment friendly adsorbent materials for fluoride removal from water [10–13].

Under the right conditions, iron oxides are strong adsorbents of anionic complexes such as AsO_4^{3-}, CrO_4^{2-} and PO_4^{3-} and organic molecules such as pesticides and humic or fulvic acids [14–17]. The granular hydrous ferric oxide plays an important role for the removal of anions from aqueous solutions [18]. Though attempts were made by different researchers for fluoride removal studies on hydrous ferric oxide [19] and activated ferric hydroxide [20], complete adsorption and desorption studies were not carried. The mixed iron oxide nano powder containing different phases (goethite (α-FeOOH), hematite (α-Fe_2O_3) and ferrihydrite ($Fe_5HO_8{\cdot}4H_2O$)) synthesised through CTAB surfactant mediation-precipitation route was also tested for fluoride removal studies [11]. Similarly, iron oxide nano powders synthesised through microemulsion route has demonstrated high adsorption capacity for fluoride from aqueous solutions [21]. Though iron oxide-based adsorbents prepared through above said methods show high surface area and high adsorption capacities for fluoride, simple methods of preparation and low cost are always preferred. The desirable characteristics of any adsorbent for defluoridation process are cost effectiveness, easy handling, fast kinetics, high adsorption capacity and reusability. The adsorption potential of iron oxides/hydroxides/oxy-hydroxides by adsorption or by incorporation within the bulk depends on their behaviour during three major stages; their initial formation by precipitation or co-precipitation, their transformation to a more stable phase, and their susceptibility to dissolve or to ex-solve incorporated trace components.

In the present study, pure ferric hydroxide was synthesised under optimised experimental conditions by simple wet chemical method. The material was characterised and investigated for its fluoride removal efficiency from water by conducting batch adsorption and desorption experiments. The material was then tested for fluoride removal from groundwater samples at natural pH conditions and the results are discussed.

2. Experimental methods

2.1. Materials

The chemicals used in the preparation of ferric hydroxide were as follows: $Fe(NO_3)_3{\cdot}9H_2O$ and KOH. For fluoride adsorption and desorption experiments, stock fluoride solution (100 mg/L) was prepared by dissolving sodium fluoride (NaF) in double-distilled water. For adjusting solution pH, dilute alkali or dilute acid were used. SPADNS reagent (sodium 2-(para sulfo phenyl azo)-1,8-dihydroxy-3,6-naphthalene disulfonate) and zirconyl oxychloride were used for fluoride estimation by colorimetric method. All these chemicals were of GR (guaranteed reagent) grade and procured from E. Merck, India. Double-distilled water was used for preparation of the solutions and washing/rinsing purpose.

2.2. Synthesis of $Fe(OH)_3$

For the synthesis of ferric hydroxide, required amount of 0.1 M iron (III) nitrate ($Fe(NO_3)_3{\cdot}9H_2O$) solution was neutralised by dropwise addition of 1 M KOH solution under constant stirring till pH 7.5 was attained, and then contents were stirred for an hour and allowed to settle. The supernatant solution was separated and the precipitate was washed repeatedly with warm double distilled water in a centrifuge at 7,000–8,000 rpm. The supernatant solution was analysed for Fe content by atomic absorption spectrophotometer in order to check the completion of precipitation. The synthesised precipitate was dried in a hot air oven at 60°C until it was completely dried. The material was then powdered and stored in an airtight container for further studies.

2.3. Characterisation studies

The X-ray diffraction (XRD) patterns of the sample were taken by using P Analytical, model-X′ pert PRO PW-3040/60 with Mo K_α radiation at a scan speed of $1.2^\circ\,min^{-1}$ over a range of 5–50°. The TEM analysis of the sample was carried out on transmission electron microscope (TEM), model TECNAI G^2, FEI, the Netherlands. For Fourier transform infrared (FTIR) spectra, Varian-Australia, model 800 spectrophotometer was used. The weight loss measurements were carried out thermo gravimetrically (TG, Metler Toledo TGA/SDTA 821e, Switzerland) in dry air at a heating rate of 20°C/min. All the pH measurements were carried out using Consort digital pH meter (model 231). The pH_{pzc} of the prepared sample was determined by solid addition method [22]. Fluoride was analysed following SPADNS method using Thermo, water analyser spectrophotometer model AquaMate [23].

2.4. Fluoride adsorption and desorption studies

Fluoride adsorption experiments were conducted by batch equilibrium method. A 100 mg/L fluoride stock solution was prepared by dissolving 0.221 g of NaF in 1 L of double-distilled water. The experimental solutions were prepared by appropriate dilutions of the above solution. A 0.025 g of the sample was taken in a 100 mL polyethylene plastic vial and 50 mL of fluoride solution of known concentration was added. The solutions pH was adjusted to desired values by using 0.01 N HCl or NaOH. The contents were kept for constant shaking in a temperature-controlled Julabo water bath shaker over a period of time and the solids were separated by centrifuging at 5,000 rpm by (REMI) centrifuge. The solutions were collected for analysis and fluoride concentration in the solutions was determined. The adsorption capacity X (mg/g) of the adsorbent was calculated from the following equation $X = (C_i - C_e)/C_A$; where C_e is the residual concentration reached at equilibrium state (mg), C_i is initial fluoride concentration (mg) and C_A is the adsorbent concentration (g). For the desorption experiments, known amount of fluoride loaded ferric hydroxide sample was treated with 50 mL of NaOH at different molar strengths (0.1–0.5 M) for 8 h in a temperature-controlled water bath shaker. The contents were separated and fluoride content in the solution was estimated by following the above-mentioned procedure.

3. Results and discussion

3.1. Characterisation of amorphous $Fe(OH)_3$

The chemical analysis of the prepared ferric hydroxide showed Fe content of 56%. The estimated Brunauet–Emmett–Teller (BET) specific surface area was 231 m^2/g. This value is well comparable with the reported values in the literature, which are in the range of 160–230 m^2/g and were classified as amorphous FeOOH [24]. The pH_{PZC} of the sample was 4.8, which is much lower than the reported values for amorphous hydrous ferric oxide [22]. The literature values for point of zero charge have shown variation from 6.7 to 9.3. This may be due to method of preparation and conditions applied, which has great influence on the chemical, structural and physical properties of the iron oxides.

The TEM image of ferric hydroxide is shown in Fig. 1, which reveals that the particles are in micron range and irregular in shape and size.

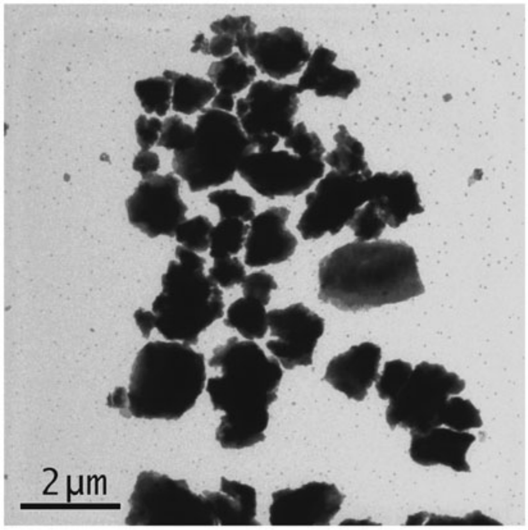

Fig. 1. TEM image of pure ferric hydroxide.

The TG-DTA traces of the prepared sample are shown in Fig. 2. The sharp endothermic peak at <100˚C indicates the evaporation of physically bound water from the surface. The total weight loss observed was around 20%, and phase transformation of $Fe(OH)_3$ to α-Fe_2O_3 was observed near 400˚C. The XRD analysis of the prepared ferric hydroxide is shown in Fig. 3(a), and it is clear that the material is poorly crystalline and showed two small peaks at 2θ values of 15.93 and 27.61 with the corresponding "*d*" spacing values of 2.53 and 1.48 A˚. The "*d*" spacing values match well for Ferric hydroxide (JCPDS No. 22-0346). The XRD of fluoride adsorbed ferric hydroxide is given in Fig. 3(b) which shows significant changes in the pattern. The

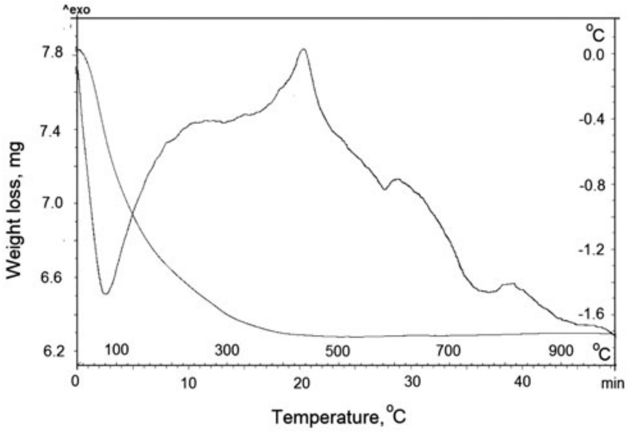

Fig. 2. Thermo gravimetric analysis (TGA) of ferric hydroxide sample.

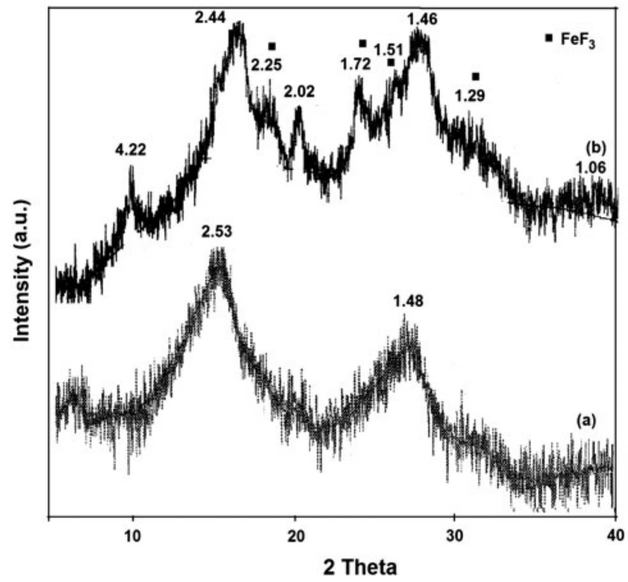

Fig. 3. XRD pattern of (a) ferric hydroxide sample prepared by co-precipitation method and (b) fluoride loaded sample.

appearance of new peaks on the ferric hydroxide surface indicates the formation of new complex (FeF_3). The fluoride loaded ferric hydroxide showed seven peaks at 2θ values of 9.64, 16.70, 18.10, 20.24, 23.73, 28.16, 31.81 and 39.12 with the corresponding *"d"* spacing values of 4.22, 2.44, 2.25, 2.02, 1.72, 1.46, 1.29 and 1.06 A°. The values match well with JCPDS No. 02–0327 and indicate the FeF_3 formation on ferric hydroxide surface.

3.2. Fluoride adsorption at different solution pH

Effect of solution pH on fluoride adsorption capacity of $Fe(OH)_3$ sample was studied by taking 25 mg of adsorbent in 50 mL of 20 mg/L fluoride solution for 4 h. The pH range studied was from 2.5 to 9.0. The results shown in Fig. 4 indicate that the fluoride adsorption is favoured at low pH values and maximum adsorption was observed at around pH 4. Similar observations were reported for fluoride adsorption onto iron containing synthetic oxy/hydroxides [25]. The pH-dependent interactions and most probable mechanisms of fluoride on metal oxide/hydroxide surface have been well discussed by many researchers [8,26]. The most probable mechanisms for fluoride adsorption on metal oxide/hydroxide surface can be depicted as [27]:

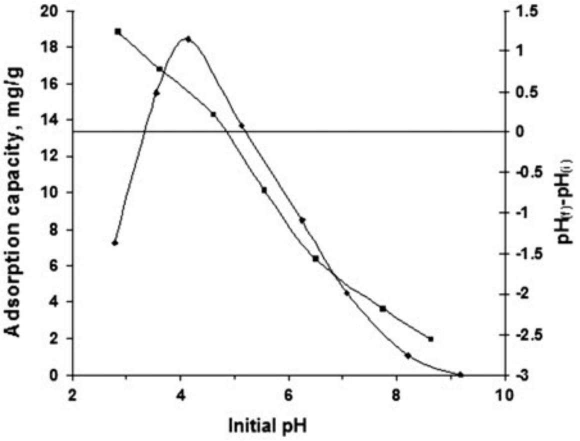

Fig. 4. Effect of solution initial pH on fluoride adsorption capacity by using amorphous ferric oxide and pHPZC plot (fluoride concentration: 20 mg/L, adsorbent: 0.5 g/L, temperature: 30°C, time: 4 h).

In acidic conditions,

$$M.xH_2O_{(\mathrm{solid})} + F^-_{(\mathrm{aq})} \leftrightarrow M.(x-1)H_2O.H^+F^-_{(\mathrm{solid})} + OH^-_{(\mathrm{aq})} \quad (1)$$

In basic conditions,

$$M.xH_2O_{(\mathrm{solid})} + X^+_{(\mathrm{aq})} + F^-_{(\mathrm{aq})} \leftrightarrow M.(x-1)H_2O.OH^-X^+F^-_{(\mathrm{solid})} + H^+_{(\mathrm{aq})} \quad (2)$$

where M is metal (iron) oxide and X^+ represents cationic species associated with F^-.

At a pH of 2–3, low fluoride removal may be due to the formation of the weakly ionised HF ($pKa = 3.2$). With increase in pH, fluoride removal increased and reached a maxima at pH 4. Further increase of pH resulted in decrease of fluoride adsorption which may be due to the competition of the hydroxyl ions with fluoride for surface sites or electrostatic repulsion of fluoride ion to the negatively charged surface. However, ferric hydroxide showed considerable adsorption in the pH range of 6–7 indicating the involvement of hydroxyl ions in fluoride removal. The adsorption mechanism of fluoride on the metal oxide surfaces was studied by many researchers and was noticed as a complicated phenomena. The nonspecific adsorption involves the columbic forces, and mainly depends on the pH_{pzc} of the adsorbent [22]. Since the zero point of surface charge on adsorbent is at pH 4.8, some hydroxyl groups are protonated at this pH, and they may adsorb anionic fluoride through electrostatic attraction. At the same time, some unprotonated hydroxyl groups can still exchange with fluoride, resulting in the release of HO^- and increase of solution pH. At higher pH beyond the isoelectric point where surface is negatively charged, only anion exchange between fluoride and hydroxyl groups is involved in the adsorption, and there by its adsorption capacity decreases.

3.3. Adsorption kinetic study

The effect of contact time was studied up to 4 h at different initial fluoride concentrations of 10, 20 and 30 mg/L. Fig. 5(a) shows a plot between contact time and fluoride adsorbed with time (q_t). It was observed that the time to achieve equilibrium is independent of fluoride initial concentration. Fluoride uptake was rapid initially, followed by a slower removal rate that gradually reached to an equilibrium condition. Almost 90% of the fluoride adsorption is achieved in the initial 60 min, and the equilibrium was observed within 120 min in all the cases.

Most widely used and simplified kinetic models namely pseudo-first-order and pseudo-second-order models have been used to study the rate and kinetics of the fluoride adsorption on ferric hydroxide surface. The linear form of pseudo-first-order rate expression of Lagergren equation is given as

$$\log(q_e - q_t) = \log q_\mathrm{e} - \frac{k_1}{2.303} t \tag{3}$$

where q_e and q_t are the amounts of fluoride adsorbed on adsorbent (mg/g) at equilibrium and at any time t (min) respectively. The plots of log ($q_e - q_t$) versus t at a fixed adsorbate and adsorbent dose, pH and temperature resulted in a straight line with good correlation coefficients (>0.98), which indicated applicability of the Eq. (3) and first-order kinetics as shown in Fig. 5(b). The rate constant k_1 and q_e (calculated) values were determined from the slope and the intercept of the plots and are given in Table 1. It is observed that though the correlation coefficients are high, the experimental and calculated q_e values show

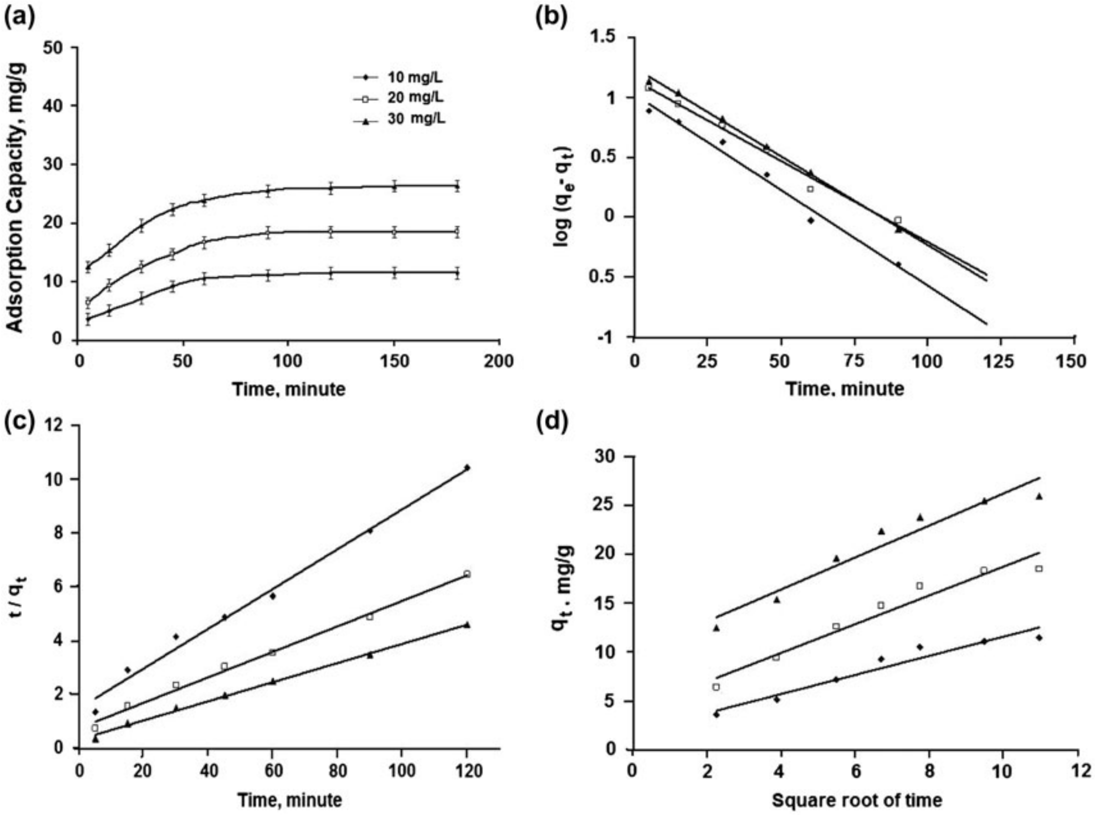

Fig. 5. (a) Effect of contact time on fluoride adsorption onto ferric hydroxide at different initial fluoride concentrations, (b) Lagergren plots, (c) second-order kinetics plots and (d) intraparticle diffusion plots (pH: 4, adsorbent: 0.5 g/L, temperature: 30˚C).

Table 1
Calculated kinetic parameters for fluoride adsorption at different initial fluoride concentrations

	Pseudo-first order			Pseudo-second order			Intra-particle diffusion	
	k_1(1/min) × 10^{-2}	q_e (mg/g)	R^2	k_2(g/mg/ min) × 10^{-2}	q_e (mg/g)	R^2	k_i (mg/g/min$^{1/2}$)	R^2
Sample FH: Experimental q_e values are 11.55, 18.50 and 26.35 mg/g for 10, 20 and 30 mg/L respectively								
10	3.66	10.65	0.98	3.61	13.00	0.98	1.63	0.93
20	3.10	14.10	0.98	2.81	21.10	0.99	1.46	0.94
30	3.40	17.75	0.98	3.34	28.24	0.99	0.97	0.93

considerable deviations; hence, the data was fitted to pseudo-second-order model, which is given as:

$$\frac{t}{q_\mathrm{t}} = \frac{1}{k_2 q_\mathrm{e}^2} + \frac{1}{q_\mathrm{e}} t \tag{4}$$

where q_e and q_t have the same meaning as mentioned above, and k_2 is the rate constant for the pseudo-second-order kinetics. The plots of t/q_t versus t are shown in Fig. 5(c). In this case, the experimental q_e values are close to the ones predicted by the pseudo-second-order model indicating good fitting of the model.

Internal diffusion is an important mass transfer process during the removal of inorganic ions by porous metal oxides/hydroxides. For the rate constant of intraparticle diffusion, the equation can be written as

$$q_\mathrm{t} = k_\mathrm{i} \sqrt{t} \tag{5}$$

where k_i is intraparticle diffusion rate constant (mg/min$^{1/2}$). In this study, possibility of existence of intraparticle diffusion was tested by plotting the graph between amount of fluoride adsorbed and square root of time. The double nature of these plots as shown in Fig. 5(d) may be explained as: the initial curve portions are attributed to boundary layer diffusion effect, while the final linear portions are due to intraparticle diffusion effect [28]. The rate constant for intra-particle diffusion coefficient k_i, was determined from slopes of linear portion of the respective plots. The linear portions of the curves do not pass the origin, this indicates that mechanism of fluoride removal on adsorbents is complex and, both the surface adsorption as well as intraparticle diffusion contribute to the rate-determining step [29]. The adsorption kinetic model parameters obtained from the above plots are also given in Table 1.

3.4. Adsorption isotherm study

The most widely employed models Langmuir and Freundlich model were used to describe the equilibrium relationship between the adsorbent and the adsorbate. The equilibrium data obtained for initial fluoride concentration variation from 5 to 30 mg/L on fluoride adsorption capacity were plotted in respective linearised forms of Langmuir and Freundlich adsorption isotherms

$$\frac{C_\mathrm{e}}{q_\mathrm{e}} = \frac{1}{Q_o b} + \frac{C_\mathrm{e}}{Q_o} \tag{6}$$

$$\log q_e = \log K_F + \frac{1}{n}\log C_e \tag{7}$$

where C_e is equilibrium concentration (mg/L), q_e is the amount adsorbed at equilibrium (mg/g), Q_o is adsorption capacity for Langmuir isotherm and "*b*" is an energy term which varies as a function of surface coverage strictly due to variations in the heat of adsorption. The Freundlich constant, "*n*" indicates the degree of favourability of adsorption and K_F is the isotherm constant [29]. The adsorption data of fluoride on ferric hydroxide fitted to both Langmuir and Freundlich isotherm models as shown in Figs. 6 (a) and (b). The calculated Langmuir isotherm parameters Q_o was found to be 35.48 mg/g and "*b*" has value of 0.20 L/mg, which indicates a low heat of adsorption. The Freundlich isotherm parameters K_F and "*n*" were found to be 7.63 and 2.17 respectively. The "*n*" values indicate the bond strength between adsorbate and adsorbent and heterogeneous nature of the ferric hydroxide surface. Some of the Langmuir adsorption capacities of iron based adsorbents reported in the literature are compared with amorphous ferric hydroxide in Table 2 and the synthesised ferric hydroxide showed much better capacity than the reported iron-based adsorbents.

3.5. Effect of competing anions

The presence of other anions on fluoride removal efficiency of ferric hydroxide was studied by taking chloride, sulphate, phosphate, arsenate, nitrate and carbonate (0–25 mg/L). Results are reported graphically in Fig. 7. It was found that the anions like sulphate, arsenate, and phosphate exert strong interference on fluoride adsorption while the

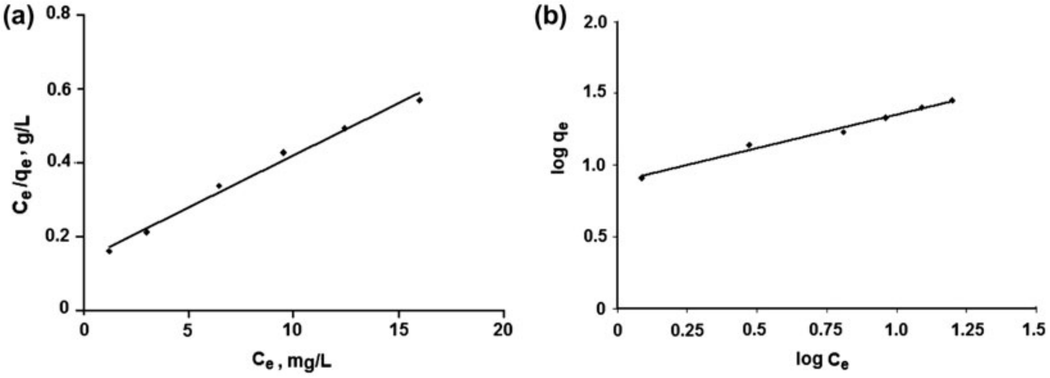

Fig. 6. (a) Langmuir adsorption isotherm and (b) Freundlich adsorption isotherm.

Table 2
Comparison of fluoride adsorption capacities of different iron based materials from the literature

Sl. No.	Adsorbent	Adsorption capacity (mg/g)	Initial [F$^-$], mg/L	Eq. time, h	pH	Reference
1	Iron(III)-tin(IV) mixed oxide	10.47	10–50	2	6.4	[34]
2	Hydrous Ferric Oxide	16.5	1–1,000	1	4.0	[20]
3	GFH**	7	1–100	24	6–7	[21]
4	Fe(III) loaded carboxylated chitosan beads	4.23	11–17	0.67	7	[35]
5	Magnetic-chitosan particles	22.49	5–140	2.5	7	[10]
6	Fe(III)-loaded ligand exchange cellulose	18.55	10–200	8	4–9	[36]
7	Synthetic siderite	1.78	20	NA	6.8	[37]
8	Amorphous ferric hydroxide	35.4	5–30	2	4.0	Present study

GFH** - granular ferric hydroxide.

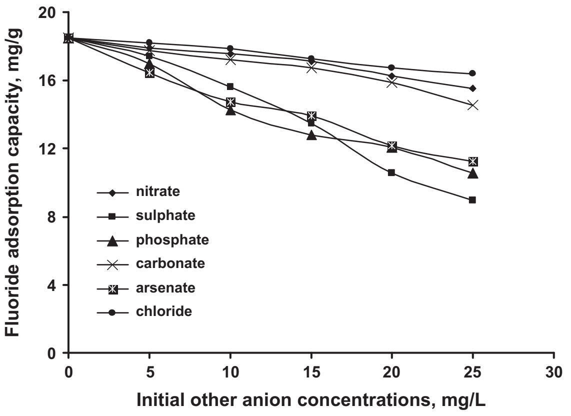

Fig. 7. Effect of other anions concentration on fluoride adsorption efficiency of amorphous ferric hydroxide (fluoride concentration 20 mg/L, adsorbent 0.5 g/L, pH: 4.0 and temperature 30˚C).

presence of nitrate, chloride and carbonate showed comparatively less interference at pH 4. The removal efficiency decreased gradually, with increase of phosphate, sulphate and arsenate concentrations, due to the fact that these ions compete with fluoride ions for the adsorption sites on ferric oxide surface. Similar findings were reported in the literature for fluoride removal studies by crystalline ferric oxide [20]. The degree of decrease in fluoride removal efficiency with increase of other anion concentration was found to be: sulphate > phosphate > arsenate > carbonate > chloride > nitrate.

3.6. Possible adsorption mechanism

The pH changes were observed during the experimentation, the pH of equilibrated solutions were increased in the acidic range and decreased in alkaline range. This indicates that the fluoride adsorption on ferrihydrite surface is a combination of both anion exchange and van der Waals forces [30]. The mechanism of fluoride interaction with ferrihydrite surface is thought to be anion exchange between fluoride and OH^- ions in acidic range. And this is supported by the rise of pH in acidic conditions. However, sample also showed adsorption at pH > 6, which indicates the involvement of van der Waals forces. The pH_{PZC} of the sample was 4.8, which holds back the movement of fluoride towards adsorbent surface due to columbic repulsion. Another reason for decrease of adsorption with increase of pH might be due to strong competition from OH^- ions to F^- on active adsorption sites.

The surface characterisation of used ferric hydroxide was carried out by XRD, FTIR and SEM EDAX analysis. The FT-IR spectrum for pure and fluoride adsorbed ferric hydroxide is shown in Fig. 8 (a) and (b). A broad absorption band at 688 cm^{-1} for pure ferric oxide in Fig. 8(a) may be due to Fe–O stretching mode [31]. The bands at 3,613 and 1,626 cm^{-1} are typical of HOH stretching and bending vibrations of water molecules. The small band at 1,384 cm^{-1} is due to residual nitrate in the sample. Visible changes were observed after fluoride adsorption on ferric hydroxide surface in Fig. 8(b).

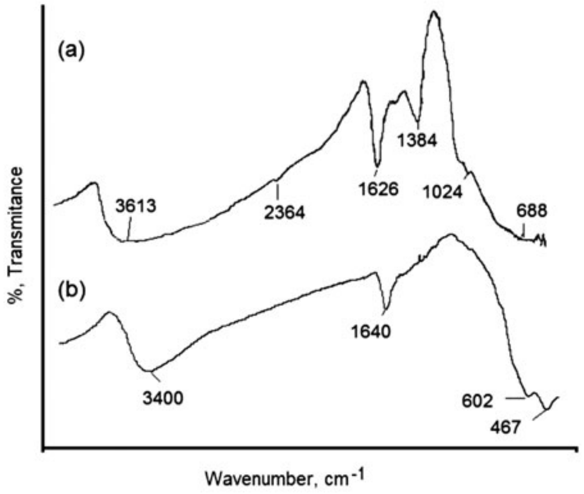

Fig. 8. FT-IR spectra of Ferric hydroxide (a) before and (b) after fluoride adsorption.

It is clearly observed that the intensity of bands at 3,613 and 1,626 cm^{-1} significantly decreased in fluoride adsorbed ferric hydroxide sample. Further, new bands at 602 and 467 cm^{-1} instead of single broad band (688 cm^{-1}) were observed indicating the formation of new bonding of Fe with fluoride. The XRD of fluoride-loaded sample had indicated the formation of FeF_3. This study supports that the fluoride interaction on ferric hydroxide surface is partly due to anion exchange.

The results obtained from SEM and energy dispersive X-ray spectroscopy (EDX) spectra of F^- adsorbed ferric hydroxide are given in Fig. 9(a) and (b). The elemental analysis of the selected portion was determined by quantitative analysis of EDX. Though there is no visible difference in ferric hydroxide surface, the SEM–EDX analysis provides direct evidence that the F^- ions are adsorbed on ferric hydroxide surface. The presence of Si in the elemental analysis of the adsorbent is due to glass sample holder.

3.7. Regeneration studies

The regeneration studies were carried out by taking known amount of fluoride bearing ferric

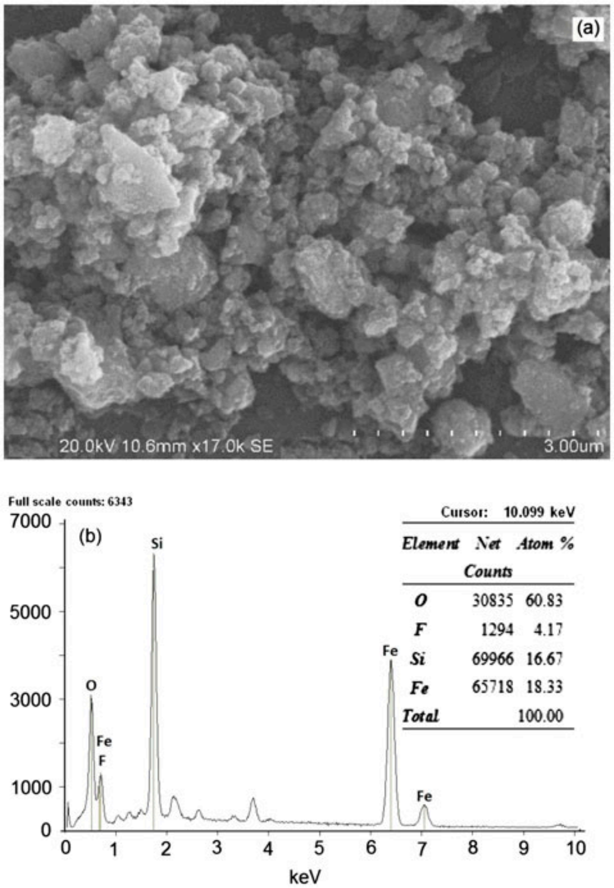

Element	Net Counts	Atom %
O	30835	60.83
F	1294	4.17
Si	69966	16.67
Fe	65718	18.33
Total		100.00

Fig. 9. (a) SEM image of ferric hydroxide after fluoride adsorption, (b) EDAX spectrum and inset of figure (b): quantitative analysis of fluoride loaded sample.

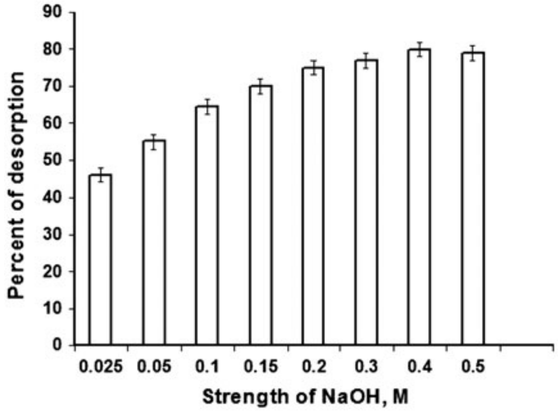

Fig. 10. Effect of NaOH strength on fluoride desorption (time 24 h, F^- loaded 26 mg/g).

hydroxide sample (37.55 mg of F^-/g) in poly propylene bottles with 25 mL of NaOH solution of different strength (0.025 to 0.5 M) for 8 h. The results show (Fig. 10) that a maximum regeneration of 75–80% could be obtained with 0.2 M NaOH, further regeneration studies with higher concentrations of NaOH solution did not show much improvement. This underlines the hypothesis of the chemical reaction between fluoride and $Fe(OH)_3$ adsorbent. Similar observations were reported in the literature for fluoride-loaded granular ferric hydroxide (showed 65% desorption) in alkaline medium with pH > 10 [30].

3.8. Removal of fluoride from groundwater

In the state of Odisha, India there are many locations where fluoride is present in excess of acceptable limits (>1 mg/L) in groundwater. For this study, water samples were collected from fluoride endemic districts Nayagarh and Khurda of Odisha. Total 5 groundwater samples were collected using clean plastic bottles from identified tube well, bore well, and dug well from fluoride endemic villages.

The physico-chemical parameters of the groundwater samples were analysed and are given in Table 3. The adsorption tests were conducted without adjusting pH and variable chosen was adsorbent dose by keeping the contact time as 2 h at ambient temperature. The fluoride content in the water samples after treatment was analysed and it was observed that the requirement of adsorbent to remove fluoride from groundwater samples was much higher when compared to their requirement for F^- removal from synthetic solutions. This is due to high pH values and presence of other competing anion concentrations in the groundwater samples. Similar observations were reported in the literature [32,33]. From these studies it was found that the ferric hydroxide could reduce F^- levels to < 1.0 mg/L from ground water samples (containing 2–5 mg/L F^-) at natural pH with dose variation of 0.3 to 1.2 g/L. The major competing anions in the groundwater samples were chloride and sulphate. The analysis of the treated water for chloride and sulphate showed considerable decrease in their concentrations (28–40%) depending on the adsorbent dose. The pH of the groundwater samples was in the range of 6.9–8.5, which is also another reason for decrease in fluoride adsorption, resulting in requirement of higher amount of adsorbent dose.

3.9. Testing of tap water spiked with fluoride

In order to ascertain whether there was any leaching of iron into the treated water, normal municipality tap water used for drinking purpose was spiked with 5 mg/L of fluoride and was treated with ferric hydroxide, at natural pH. Various water quality parameters including Fe were determined for treated

Table 3
Analysis of the groundwater samples collected from Nayagarh and Khurda districts of Odisha, India

SC[#]	Location	pH	PO_4^{3-} mg/L	F^- mg/ L	TH[*] mg/L	NO_3^- mg/L	Cl^- mg/L	SO_4^{2-} mg/L
S1	Singhpur Village, DW[**]	7.15	0.08	3.20	56.85	0.07	388.5	340
S2	Balsinghpur Village DW[**]	6.89	0.05	4.85	62.50	0.05	436.0	280
S3	Golpokhari, TW[***]	8.05	Nd	1.8	74.40	0.12	178.0	56
S4	Nilakanta Prasad village TW[***]	7.58	Nd	2.10	26.00	0.08	290.0	42
S5	Khurda, Morichia village, TW[***]	7.75	Nd	2.50	36.24	0.24	382.4	68.05

[*]TH-Total hardness; [**]DW-Dug well; [***]TW-Tube well; # Sample code; Nd-Not detected.

Table 4
Analysis of water (spiked with 5 mg/L of F^-) parameters after treatment with ferric hydroxide

Parameters	Tap water analysis before treatment	Tap water analysis after treatment (ferric oxide dose: 0.5 g/L)	Desirable limits (BIS 10,500:1991)
pH	6.80	6.62	6.5–8.5
Total hardness, mg/L	79	77	300
NO_3^-, mg/L	0.02	nd	45
Cl^-, mg/L	42.8	38.5	250
F^- (added), mg/L	5.0	0.85	1.0
Fe, mg/L	0.17	0.21	0.3

and untreated water and the results are presented in Table 4. It is evident from the results that the parameters of the water after fluoride removal remained almost unaltered with slight change in pH. Most importantly Fe analysis of treated water confirmed that there was no dissolution of Fe ions into water during the treatment. The values of various water quality parameters were compared with Indian Standard for drinking water [3] and it was found that most of the values were within the permissible limits indicating that use of ferric hydroxide for treatment of fluoride-contaminated drinking water is safe.

4. Conclusions

In the present study, ferric hydroxide was synthesised, characterised and studied for its fluoride removal efficiency from fluoride contaminated groundwaters. The sample showed BET surface area of 231 m^2/g and exhibited encouraging results for fluoride removal from water. The following conclusions can be drawn from the above studies:

(1) The adsorption of fluoride ions on amorphous ferric hydroxide is highly pH-dependent. The optimum pH is in the range of 4–5, there after it showed decreasing trend for fluoride adsorption capacity.
(2) The fluoride adsorption proceeded through complex mechanism involving ion exchange and complexation at the surface. Formation of new compound FeF_3 was confirmed by XRD. FTIR spectrum of loaded sample showed additional bands when compared to the spectra of as-such ferric hydroxide.
(3) The material showed maximum fluoride adsorption capacity of 35.44 mg/g at pH 4. The fluoride-loaded ferric hydroxide can be regenerated (75–80%) with 0.2 M NaOH for reuse.
(4) Fluoride-containing groundwater treatment studies under natural conditions were found to be encouraging. Ferric hydroxide could reduce F^- levels to < 1.0 mg/L from groundwater samples (containing 2–5 mg/L F^-) at natural pH with dose variation of 0.3–1.2 g/L.
(5) The tap water spiked with 5 mg/L fluoride was used to determine the solubility of iron ions during the fluoride removal process at neutral pH. The residual concentration of fluoride was < 1 mg/L and the concentration of iron ions also met the standards of potable water.
(6) Taking into account the high adsorption capacity and the low residual amount of fluoride in the water, ferric hydroxide can be suitable adsorbent to treat fluoride contaminated water to attain drinking standard quality.

Acknowledgement

Authors wish to thank the Director, CSIR-Institute of Minerals and Materials Technology for giving permission to publish this work and central characterisation cell, CSIR-IMMT for characterisation of the samples. Funding the work by CSIR through CSC0101 is acknowledged.

References

[1] www.unicef.org/wes/files/fluoride.pdf. Fluoride in water: An overview, information supply by UNICEF India.

[2] WHO, Guidelines for Drinking Water Quality, Health criteria and other supporting information, 2nd ed., World Health Organisation, Geneva, 2 1996 pp. 231–237.

[3] BIS, Bureau of Indian Standards Drinking water-specification, IS:10500, New Delhi, 2003.

[4] M. Hichour, F. Persin, J. Sandeaux, C. Gavach, Fluoride removal from waters by Donnan dialysis, Sep. Purif. Technol. 18 (2000) 1–11.

[5] F. Lou, K. Inoue, The removal of fluoride ion by using metal (III)-loaded amberlite resins, Solvent Extr. Ion Exch. 22 (2004) 305–322.

[6] P.I. Ndiaye, P. Moulin, L. Dominguez, J.C. Millet, F. Charbit, Removal of fluoride from electronic industrial effluent by RO membrane separation, Desalination 173 (2005) 25–32.

[7] M.G. Sujana, G. Soma, N. Vasumathi, S. Anand, Studies on fluoride adsorption capacities of amorphous Fe/Al mixed hydroxides from aqueous solutions, J. Fluorine Chem. 130 (392) (2009) 749–754.

[8] A.M. Raichur, M.J. Basu, Adsorption of fluoride onto mixed rare earth oxides, Sep. Purif. Technol. 24 (2001) 121–127.

[9] Y.C. Wu, A. Nitya, Water defluoridation with activated alumina, J. Environ. Eng. ASCE 105 (1979) 357–367.

[10] Y.-H. Huang, Y.-J. Shih, C.-C. Chang, Adsorption of fluoride by waste iron oxide: The effects of solution pH, major coexisting anions, and adsorbent calcination temperature, J. Hazard. Mater. 186 (2011) 1355–1359.

[11] M. Mohapatra, K. Rout, P. Singh, S. Anand, S. Layek, H.C. Verma, B.K. Mishra, Fluoride adsorption studies on mixed-phase nano iron oxides prepared by surfactant mediation-precipitation technique, J. Hazard. Mater. 186 (2011) 1751–1757.

[12] L. Chen, H-X. Wu, T-J Wang, Y. Jin, Yu Zhang, X-M. Dou, Granulation of Fe-Al-Ce nano-adsorbent for fluoride removal from drinking water by spray coating on sand in a fluidized bed, Powder Tech. 193 (2009) 59–64.

[13] X. Zhao, J. Wang, F. Wu, T. Wang, Y. Cai, Y. Shi, G. Jiang, Removal of fluoride from aqueous media by $Fe_3O_4@Al(OH)_3$ magnetic nanoparticles, J. Hazard. Mater. 173 (2010) 102–109.

[14] S.R. Randall, D.M. Sherman, K.V. Ragnarsdottir, Sorption of As(V) on green rust($Fe_4(II)Fe_2(III)(OH)_{12}SO_4.3H_2O$) and lepidocrocite (gamma-FeOOH): surface complexes from EXAFS spectroscopy, Geochim. Cosmochim. Acta 65 (2001) 1015–1023.

[15] M. Ding, B.H.W.S. de Jang, S.J. Roosendaal, A. Vredenburg, XPS studies on the electronic structure of bonding between solid and solute; adsorption of arsenate, chromate, phosphate, Pb^{2+}, and Zn^{2+} ions on amorphous black ferric oxyhydroxide, Geochim. Cosmochim. Acta 65 (2000) 1209–1219.

[16] L. Clausen, I. Fabricius, Atrazine, isoproturon, mecoprop, 2,4-D, and bentazone adsorption onto iron oxides, J. Environ. Qual. 30 (2001) 858–869.

[17] Q.H. Zhou, P.A. Maurice, S.E. Cabaniss, Size fractionation upon adsorption of fulvic acid on goethite: Equilibrium and kinetic studies, Geochim. Acta. 65 (2001) 803–812.

[18] E. Kumar, A. Bhatnagar, M. Ji, W. Jung, S.-H. Lee, S.-J. Kim, G. Lee, H. Song, J.-Y. Choie, J.-S. Yang, B.-H. Jeon, Defluoridation from aqueous solutions by granular ferric hydroxide (GFH), Water Res. 43 (2009) 490–498.

[19] S. Dey, S. Goswami, U.C. Ghosh, Hydrous ferric oxide for contaminated water, Water Air Soil Pollut. 158 (2004) 311–323.

[20] X. Huang, W. Ding, An Activated Ferric Hydroxides Adsorbent for Water Treatment and its Preparation Method, China patent No. 03153998 X, 2005 (in Chinese).

[21] M.G. Sujana, S. Mohanty, Characterization and fluoride uptake studies of nano-scale iron oxide-hydroxide synthesized by microemulsion method, Int. J. Eng. Sci. Technol. (IJEST) 2(8) (2010) 1–12.

[22] L.S. Balistrieri, J.W. Murray, The surface chemistry of goethite (alpha FeOOH) in major ion seawater, J. Am. Sci. 281 (1981) 788–806.

[23] E. Arlond, Greenberg, S. Lenore Coesreri, D. Andrew, Eaton (Eds.), Standard Methods for the Examination of Water and Waste Water, John Willey, New York, 1987, p. 325.

[24] C. Fuller, C. Davis, G.A. Waychunas, Surface chemistry of ferrihydrite-Part - 2, kinetics of arsenic adsorption and co-precipitation, Geochim. Cosmochim. Acta 57 (1993) 2271–2282.

[25] Y.-H. Huang, Y.-J. Shih, C.-C. Chang, Adsorption of fluoride by waste iron oxide: The effects of solution pH, major coexisting anions, and adsorbent calcination temperature, J. Hazard. Mater. 186 (2011) 1355–1359.

[26] H.-X. Wu, T.-J. Wang, L. Chen, J. Yong, The roles of the surface charge and hydroxyl group on a Fe-Al-Ce adsorbent in fluoride adsorption, Ind. Eng. Chem. Res. 48 (2009) 4530–4534.

[27] D.M. Ruthven, Principles of Sorption and Sorption Processes, Wiley, New York, 1984 (Chapter 6).

[28] G. McKay, M.J. Bino, Fixed bed adsorption for the removal of pollutants from water, Environ. Pollut. 66 (1990) 33–53.

[29] M. Mahramanlioglu, I. Kizilcikli, I.O. Bicer, Sorption of fluoride from aqueous solution by acid treated spent bleaching earth, J. Fluorine Chem. 115 (2002) 41–47.

[30] Y. Tang, X. Guan, J. Wang, N. Gao, R.M. Martin, C.C. Charles, Fluoride adsorption onto granular ferric hydroxide: Effects of ionic strength, pH, surface loading, and major co-existing anions, J. Hazard. Mater. 171 (2009) 774–779.

[31] M. Yamaura, R.L. Camilo, L.C. Sampaio, M.A. Macêdo, M. Nakamura, H.E. Toma, Preparation and characterization of (3-aminopropyl) triethoxysilane-coated magnetite nanoparticles, J. Magn. Magn. Mater. 279(2–3) (2004) 210–217.

[32] Y. Ku, C. Hwei-Mei, W. Wen, The removal of fluoride ion from aqueous solution by a cation synthetic resin, Sep. Sci. Technol. 37(1) (2002) 89–103.

[33] P.C. Zhang, D.L. Spark, Kinetics and mechanisms of sulphate adsorption/desorption on goethite using pressure-jump relaxation, Soil Sci. Soc. Am. J. 54 (1990) 1266–1273.

[34] K. Biswas, D. Bandhoyapadhyay, U.C. Ghosh, Adsorption kinetics of fluoride on iron (III)–zirconium(IV) hybrid oxide, Adsorption 13 (2007) 83–94.

[35] N. Viswanathan, S. Meenakshi, Selective sorption of fluoride using Fe(III) loaded carboxylated chitosan beads, J. Fluorine Chem. 129 (2008) 645–653.

[36] A. Eskandarpour, M.S. Onyango, A. Ochieng, S. Asai, Removal of fluoride ions from aqueous solutions by using Schwertmannite, J. Hazard. Mater. 152 (2008) 571–579.

[37] L. Qiong, G. Huaming, S. Yue, Adsorption of fluoride on synthetic siderite from aqueous solution, J. Fluorine Chem. 131 (2010) 635–641.